

Geometrical Determination of Maximum Power Point of a Photovoltaic Cell

Mehmet Goksu
Millersville University of Pennsylvania
mehmet.goksu@millersville.edu

Faruk Yildiz
Sam Houston State University
fx001@shsu.edu

Abstract

Renewable energy is one of the most important topics in energy production today due to increasing world's energy needs and global warming. An increase use of photovoltaic (PV) cells is essential for meeting this need since sunlight is clean, abundant, and effectively limitless. In this paper, a new algorithm is presented in order to determine the maximum power point (MPP) of a PV cell based on geometry of a current-voltage (I-V) curve. Even though a PV cell may be operated at any point on the I-V curve, the MPP indicates a point where the maximum power output is obtained from the cell. It is therefore necessary to accurately determine the MPP of the cells. This method also shows that geometrical construction of the MPP is independent of the characteristic of PV cells.

Introduction

It is clear that fossil fuel resources are finite and depletion will happen sooner or later. If the current level of fossil fuel energy consumption continues, the entire world's fossil fuel energy reserve will be depleted in about 100 years [1]. Fossil fuel resources will eventually be replaced by renewable energy sources, especially by solar energy. Currently, only a small portion of the world's energy consumption is produced by renewable energy. There is an increasing demand for clean, renewable energy as the world's fossil fuel reserves continue to diminish. Scientists and engineers are trying to make renewable energy a more viable and cost-effective method of generating electricity in an effort to partially fulfill the world's energy needs.

I-V and power versus voltage (P-V) characteristics of PV cells have been studied extensively over the last decade. Some simulations of PV cells have been primarily made to develop an algorithm in order to determine precisely the location of the MPP while it is operating. The location of the MPP continually changes as the environmental condition of the PV cell changes. To extract maximum power from a PV cell in any weather condition, an MPP controller is used in the system. An MPP controller is a device that uses either a logical or mathematical algorithm in order to operate the PV cell at the maximum efficiency under varying weather condition and loads. There are many MPP controller algorithms reported in the literature [2-5]. These algorithms vary in control strategies, variables, and hardware

implementation. Each algorithm has its own unique property, with advantages and disadvantages with respect to these parameters [6-10].

The perturb-and-observe (P&O) and incremental conductance (INC) algorithms are the most widely used methods in MPP controllers. A P&O algorithm periodically compares power at different steps by perturbing voltage and current. This process continues until the MPP is reached. Even though this algorithm is one of the simplest to implement, a P&O algorithm suffers from slow dynamic response [11] and oscillation around the MPP due to loss in power [12] in a rapidly changing weather condition.

An INC algorithm uses the conductance of the P-V curve [13]. Similarly, this algorithm compares the instantaneous conductance and the perturbed conductance. Comparison between these conductance values is used to determine the location of the MPP. To improve the response time reaching the MPP, an INC algorithm in the perturbation uses variable step size instead of fixed step for tracking the MPP [14].

The MPP algorithms used to determine the location of the MPP require some physical parameters related to the PV cells. Also, some algorithms use higher levels of computational analysis. In the present work, a new and simple method is explained to determine the location of the MPP on the I-V curve. This method does not require any mathematical computation or knowledge about the PV cell. Kumar and Pachal [15] presented the geometrical prediction of the MPP by forming a parallelogram on the I-V characteristic curve. The method described in their work requires different values of voltage and current on the I-V curve, including the short circuit current and open circuit voltage, in order to construct the parallelogram. After forming the parallelogram, the Lagrangian interpolation method is used to determine precisely the location of the MPP. These authors presented their work in another study to predict the location of the MPP based on quadratic regression analysis of the geometry on the P-V characteristic curve [16]. The proposed new method presents the geometrical location of the MPP in a very straight-forward fashion without using any characteristics of the PV cell. With this method, it is shown that the location of the MPP is independent of the characteristics. It is also applicable to any types of the PV cells in any environmental condition.

Theory

In the present paper, the geometrical location of the MPP on the I-V curve is described using the fact that the maximum of a function is obtained by setting the differential of the function to zero. Figure 1 shows the nonlinear I-V characteristic curve of a PV cell. The I-V curve represents the possible voltage and current operating points of the PV cell that depend mainly on solar insolation, temperature of the cell, and the partial shading condition. A PV cell produces maximum power only at a single point along the I-V curve at a specific condition. Also, the maximum power delivered by a PV cell is given by the largest rectangle fitting under the I-V curve.

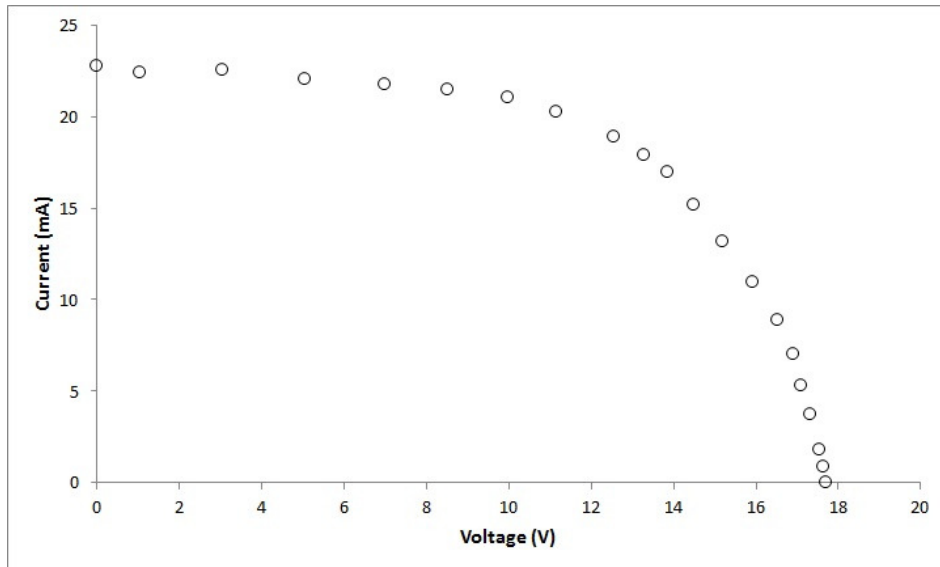


Figure 1. I-V Characteristic Curve of the PV Cell

The P-V characteristic of the cell is plotted with the I-V curve in Figure 2. The operating voltage and current at the MPP are called maximum power point voltage and current, respectively.

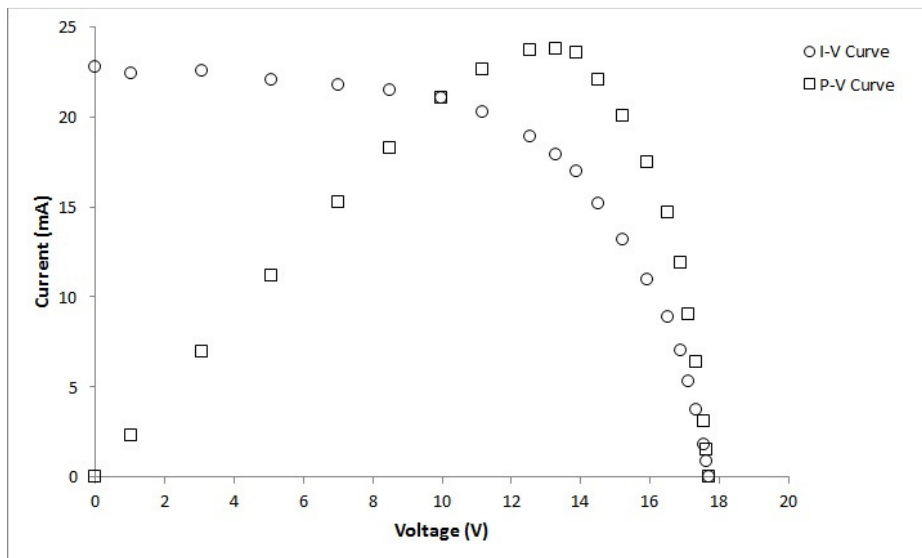


Figure 2. I-V and P-V Characteristic Curves

The MPP of a PV cell is usually located at the knee of the I-V curve where the product of current and voltage is maximum. The condition for the maximum power yields that derivative of power with respect to voltage is zero.

$$\frac{dP}{dV} = 0 \quad (1)$$

Where power is a function of voltage and current and it is defined as

$$P = P(I, V) = I \cdot V \quad (2)$$

Differentiating both sides of the equation, we can write

$$\frac{dP}{dV} = I \cdot \frac{dV}{dV} + V \cdot \frac{dI}{dV} = I + V \cdot \frac{dI}{dV} = 0 \quad (3)$$

and rearranging the equation at the MPP gives

$$\left(\frac{I}{V}\right)_{mp} = -\left(\frac{dI}{dV}\right)_{mp} \quad (4)$$

The right-hand side of the equation represents the tangent to the MPP on the I-V curve. The left-hand side of the equation represents the slope of a line that connects the coordinate origin and the MPP. This relationship is illustrated geometrically in Figure 3. From the geometrical construction, Equation (4) can be viewed in two different ways in order to describe the location of the MPP in the figure:

1. The MPP occurs on the knee of the I-V curve where the I-V line and the I-V tangent both make the same angle, α , with the horizontal V-axis, as shown in Figure 3.
2. At the MPP, the tangent to the characteristic curve makes the same angle β with a vertical line to V_{mp} as the line connecting the origin and the MPP.

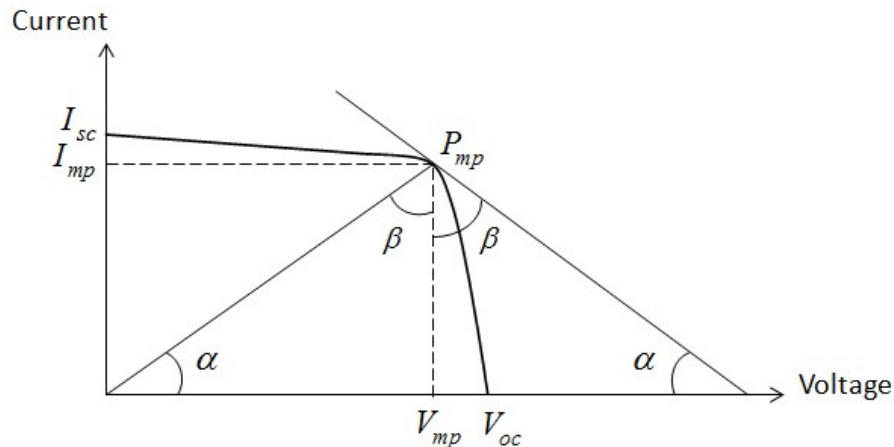


Figure 3. The Geometry of the MPP on the I-V curve.

This paper presents a new interpretation of Equation 1 that is different than all of the algorithms reported in other literature. The same mathematical condition is used in some MPP controller devices, such as INC, which compare the instantaneous conductance and the perturbed conductance. Other MPP controllers are based on the fact that the sign of derivative of power with respect to voltage changes from positive to negative when the

operating point of a PV cell changes from the left- hand side of the MPP to the right- hand side of the MPP.

Analysis

The theory of the algorithm is tested using two different types of solar panels: a 5-W multicrystalline solar panel from Clean Dependable Technology (CDT) and a 255-W monocrystalline solar panel from Perlight Solar (PLM-255M-60). Table 1 shows the parameters of the panels from the manufacturers’ data sheets. The 5-W CDT panel was physically used in the laboratory to obtain the temperature and light intensity dependence of the I-V curves in order to test the algorithm described in the paper. On the other hand, the 255-W panel was tested using the I-V curves provided by the manufacturer of the panel [17].

Table 1. Specifications of Solar Panels

| Parameters | 5-W CDT Panel (Multicrystalline) | 255-W Perlight Panel (Monocrystalline) |
|--------------|----------------------------------|--|
| I_{sc} (A) | 0.32 | 9.05 |
| V_{oc} (V) | 21.01 | 37.20 |
| P_{mp} (W) | 5.18 | 255 |
| I_{mp} (A) | 0.31 | 8.17 |
| V_{mp} (V) | 16.68 | 31.20 |

Figure 4 shows the I-V characteristics of the 5-W solar panel. The light intensities used in the experiments are 200.0 W/m², 400.0 W/m², 600.0 W/m², and 800.0 W/m² at a temperature of 22.0 °C. A light sensor from Vernier Software & Technology (LS-BTA) was used to measure the light intensity in the experiment.

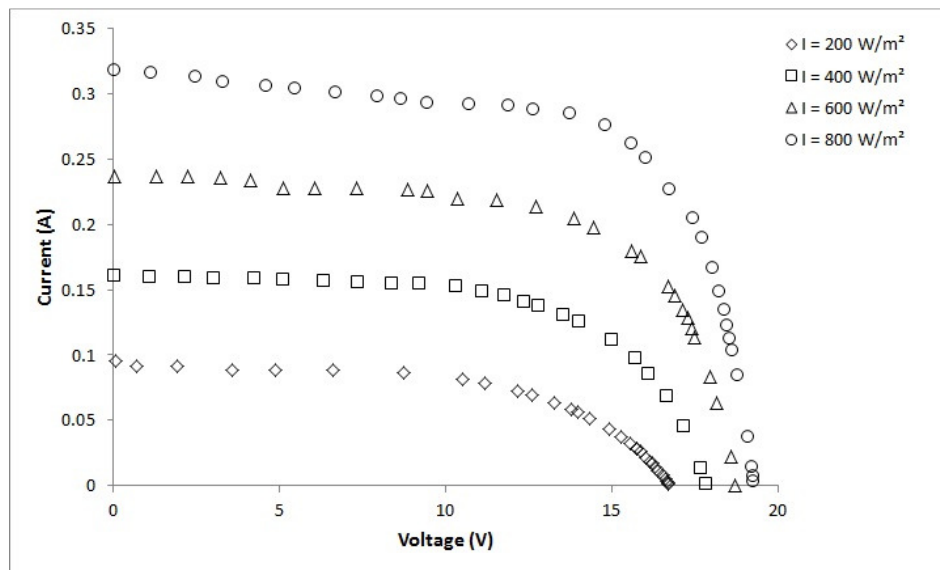


Figure 4. The Intensity Dependence of I-V Curves.

Figure 5 represents the temperature dependence of the I-V curve. The 5-W solar panel was tested at a fixed light intensity of 900.0 W/m^2 and temperatures of $14.0 \text{ }^\circ\text{C}$, $24.0 \text{ }^\circ\text{C}$, $46.7 \text{ }^\circ\text{C}$, and $54.0 \text{ }^\circ\text{C}$. An infrared thermometer (FLUKE 62-Max) was used to measure the temperature of the cell. It is important to emphasize that as the temperature of the solar panel increases, the size of the energy gap between the conduction and valance bands decreases. This decrease in the energy gap allows photons with longer wavelengths and lower energy to be absorbed by the solar panel. As a result, the short circuit current of the solar panel increases. This is a signature of the semiconductors used in the PV cells. Due to the scaling of Figure 5, it is difficult to see the increase in the current.

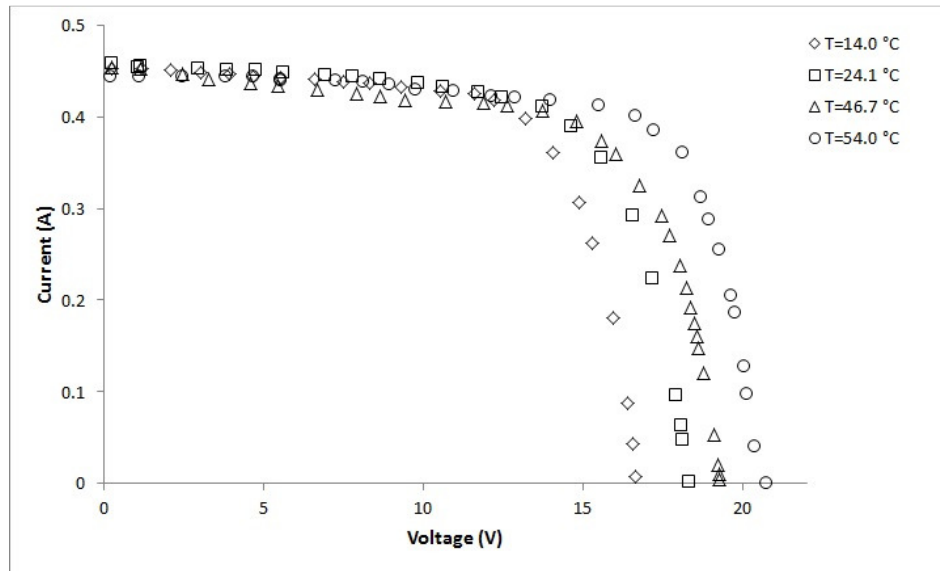


Figure 5. The Temperature Dependence of I-V Curves.

Tables 2 and 3 illustrate the average of experimental angle measurements, α and β , based on the algorithm. Each average in the tables represents the average of two angle measurements at a specified condition. The estimated uncertainty in the measurements is 0.2° . As illustrated in the tables, the average angles are different for the same panel at different conditions. It is also true that angles might be different for different panels at the same condition of radiation intensity or temperature. However, the theoretical sum of angles, α and β , should be 90° . The sum is independent of any parameters as long as angles are measured as described in the algorithm. The experimental sum of angles at different light intensities are $(90.3 \pm 0.4)^\circ$ and $(90.4 \pm 0.5)^\circ$ for the 5-W CDT panel and 255-W PML panel, respectively. Similar results are obtained at different temperatures: $(89.7 \pm 0.6)^\circ$ for the 5-W CDT panel and $(90.3 \pm 0.5)^\circ$ for the 255-W PML panel.

The experiment also reveals that the algorithm described to determine the location of the MPP based on angle measurements appears to be independent of the type of the solar panel. It should be valid for any PV cell.

Table 2. Angle Measurements at Different Intensities

| Intensity (W/m ²) | 5W Panel | | Intensity (W/m ²) | 255W Panel | |
|----------------------------------|--------------------|-------------------|----------------------------------|--------------------|-------------------|
| | α_{ave} (°) | β_{ave} (°) | | α_{ave} (°) | β_{ave} (°) |
| 200 | 12.2 | 78.6 | 200 | 8.2 | 82.6 |
| 400 | 21.2 | 69.2 | 400 | 15.8 | 74.8 |
| 600 | 24.8 | 65.4 | 600 | 23.2 | 67.6 |
| 800 | 28.2 | 62.6 | 800 | 29.0 | 61.4 |
| | | | 1000 | 35.2 | 54.2 |

Table 3. Angle Measurements at Different Temperatures

| Temperature (°C) | 5-W Panel | | Temperature (°C) | 255-W Panel | |
|---------------------|--------------------|-------------------|---------------------|--------------------|-------------------|
| | α_{ave} (°) | β_{ave} (°) | | α_{ave} (°) | β_{ave} (°) |
| 14.0 | 28.8 | 60.8 | 10 | 32.2 | 58.4 |
| 24.1 | 31.6 | 59.0 | 25 | 34.6 | 56.0 |
| 46.7 | 33.4 | 56.0 | 40 | 35.4 | 54.4 |
| 54.0 | 36.5 | 52.8 | 55 | 38.6 | 52.2 |
| | | | 70 | 40.0 | 49.8 |

Conclusion

In this study, we presented a new simple algorithm that explains the geometrical location of the MPP on the I-V curve. The proposed method is applied to two different kinds of solar panels under different light intensities and temperatures. The sum of angles in the algorithm is 90°. The experimental results clearly support the theory of algorithm that this method can be applied to any PV cell technology at any fixed environmental condition. The algorithm described in the paper could be easily implemented in any MPP controller device to operate the PV cell at the MPP under varying weather conditions.

Acknowledgements

The authors wish to acknowledge Dr. Michael Nolan for helpful conversations.

References

- [1] U.S. Energy Information Administration. (2015) EIA, Annual Energy Outlook with Projections to 2040.
- [2] Eltawil M. A. & Zhao, A. (2013). MPPT Techniques for Photovoltaic Applications. *Renewable and Sustainable Energy Reviews*. 25, 793-813.
- [3] Hussain, K. H., Muta, I., Hoshiono, T., Osakada, M. (1995). Maximum Photovoltaic Power Tracking: An Algorithm for Rapidly Changing Atmospheric Condition. *IEEE Proceeding: Generation, Transmission, and Distribution*. 142(1), 59-64.

- [4] Casadei, D, Grandi, G., Rossi, C. (2006). Single-Phase-Stage Photovoltaic Generation System Based on a Ripple Correlation Control Maximum Power Point Tracking. *IEEE Transactions on Energy Conversion*. 21(2), 562-568.
- [5] Bhatnagar, P. & Nema, R. K. (2013). Maximum Power Point Tracking Control Techniques: State-of-the-Art in Photovoltaic Applications. *Renewable and Sustainable Energy Reviews*. 22, 224-241.
- [6] ESRAM, T. & Chapman, P.L. (2007). Comparison of Photovoltaic Array Maximum Power Point Tracking Techniques. *IEEE Transactions on Energy Conversion*. 22(2), 439- 449.
- [7] Dolara, A. Faranda, Leva, S. (2009). Energy Comparison of Seven MPPT Techniques for PV Systems. *Journal of Electromagnetic Analysis and Applications*. 1(3),152-162.
- [8] Tofoli, F. L., Pereira, D. C., Paula, W. J., (2013). Comparative Study of Maximum Power point Tracking Techniques for Photovoltaic Systems. *International Journal of Photoenergy*. 2015, 1-10.
- [9] Bhatnagar, A. P. & Nema, B. R. K. (2013). Conventional and Global Maximum Power Point Tracking Techniques in Photovoltaic Application: A Review. *Journal of Renewable and Sustainable Energy*. 5(3), p032701-22.
- [10] Subudhi, B. & Pradhan R., (2013). A Comparative Study of Maximum Power Point Tracking Techniques for Photovoltaic Power Systems. *IEEE Transactions on Sustainable Energy*. 4(1), 89-98.
- [11] Femia, N., Petrone G., Spagnuolo G., Vitelli M. (2005). Optimization of Perturb and Observe Maximum Power Point Tracking Method. *IEEE Transactions on Power Electronics*. 20(4), 963-973.
- [12] Chung, H. S-K., Tse, K. K., Hui, S. Y., Mok C. M., Ho, M.T. (2003). A novel Maximum Power Point Tracking Techniques for Solar Panels Using a SEPIC or Cuk Converter. , *IEEE Transactions on Power Electronics*. 18(3), 717-725.
- [13] Koizumi, H. & Kurokawa, K. (2005) A Novel Maximum Power Point Tracking Method for PV Module Integrated Converter. *IEEE Power Electronics Specialist Conference., Conf 66*, 2081-2086.
- [14] Liu, F., Duan, S., Liu, F., Liu, B., Kang, Y. (2008). A Variable Step Size INC MPPT Method for PV System. *IEEE Transactions on Industrial Electronics*. 55(7), 2622-2628.
- [15] Kumar, G. & Pachal A. K. (2014). Geometrical Prediction of Maximum Power Point for Photovoltaics. *Applied Energy*. 119, 237-245.
- [16] Kumar, G., Trivedi, M. B., Pachal A. K. (2015). Innovative and Precise Estimation Using P-V curve Geometry for Photovoltaics. *Applied Energy*. 138, 640-647.
- [17] Perlight Solar. (n.d.). Retrieved May 10, 2016, from <http://www.perlight.com/images/pdf/plm-m-60-series-spec-sheet.pdf>

Biographies

MEHMET I. GOKSU is an Associate Professor of Physics at Millersville University of Pennsylvania. He is a condensed matter experimentalist with extensive experience in low temperature physics. His research interests include quantum computing, physics education,

and renewable energy. He has a strong interest in sustainability and energy related issues are his passion. Dr. Goksu may be reached at mehmet.goksu@millersville.edu.

FARUK YILDIZ is currently an Associate Professor of Engineering Technology at Sam Houston State University. His primary teaching areas are Electronics, Computer Aided Design, and Alternative Energy Technologies. Research interests include: low power energy harvesting, conversion, and storage, renewable energy education and technologies. Dr. Yildiz can be reached at fx001@shsu.edu.